MYOSIN SUBFRAGMENT BINDING FOR THE LOCALIZATION OF ACTIN-LIKE MICROFILAMENTS IN CULTURED CELLS

A Light and Electron Microscope Study

JEFFERY A. SCHLOSS, AMY MILSTED, and ROBERT D. GOLDMAN

From the Department of Biological Sciences, Mellon Institute of Science, Carnegie-Mellon University, Pittsburgh, Pennsylvania 15213

ABSTRACT

Fluorescein-labeled heavy meromyosin subfragment-1 (F-S-1) has been purified by ion exchange chromatography and characterized in terms of its ability to bind specifically to actin. F-S-1 activates the Mg^{++}-adenosine triphosphatase activity of rabbit skeletal muscle actin and decorates actin as shown by negative stains and thin sections of rabbit actin and rat embryo cell microfilament bundles, respectively. Binding of F-S-1 to cellular structures is prevented by pyrophosphate and by competition with excess unlabeled S-1.

The F-S-1 is used in light microscope studies to determine the distribution of actin-containing structures in interphase and mitotic rat embryo and rat kangaroo cells. Interphase cells display the familiar pattern of fluorescent stress fibers. Chromosome-to-pole fibers are fluorescent in mitotic cells.

The glycerol extraction procedures employed provide an opportunity to examine cells prepared in an identical manner by light and electron microscopy. The latter technique reveals that actin-like microfilaments are identifiable in spindles of glycerinated cells before and after addition of S-1 or HMM. In some cases, microfilaments appear to be closely associated with spindle microtubules. Comparison of the light and electron microscope results aids in the evaluation of the fluorescent myosin fragment technique and provides further evidence for possible structural and functional roles of actin in the mitotic apparatus.

KEY WORDS   microfilaments   ·   HMM   subfragment-1   ·   cultured cells   ·   actin   ·   mitotic spindle   ·   fluorescence microscopy

Determination of the distribution and organization of actin-like microfilaments in nonmuscle cells is an important approach to discerning the mechanisms of cellular motility (see references 40 and 41 for reviews). Microfilaments are identified in cells fixed and thin-sectioned for electron microscopy by their size (~6 nm diameter) and ability to bind the myosin fragments heavy meromyosin (HMM) and HMM subfragment-1 (S-1), resulting in "arrowhead" configurations or decorated complexes (26, 27, 18). This reaction is considered to be specific for actin, as HMM and S-1 do not decorate other fibrous structures in the cell (27, 19, 40).

Over the past 7-8 yr, conventional thin-sectioning techniques have been used to reconstruct the intracellular distribution and organization of microfilaments. Light microscope techniques have

also been employed to study the overall distribution of structures thought to contain actin (5). However, the supramolecular organization of actin cannot be determined by these techniques because of the limits of resolution of the light microscope (22). Only a few attempts have been made to correlate directly information from light and electron microscope studies. For instance, the distribution of phase-dense stress fibers (5) and birefringent fibers seen with polarized light microscopy (17) has been shown to correspond to that of microfilament bundles in several cultured animal cells (20, 22).

Fluorescein-labeled HMM (F-HMM), S-1 (F-S-1), and antiactin antibody in indirect immunofluorescence studies have been shown to stain stress fibers in extensively spread cells which correspond to microfilament bundles (45, 47, 22, 29, 20). We have shown that comparison of light and electron microscope data is required for the interpretation of results obtained from fluorescence microscopy. This was demonstrated by experiments in which some types of cells exhibited uniform fluorescence without showing distinct fluorescent fibers, indicating that microfilament bundles might not be present. However, the same cells have numerous microfilament bundles when examined by electron microscopy (22).

Evidence for an actin component in the mitotic apparatus obtained by F-HMM was first provided by Aronson (1). Actin-like microfilaments in mitotic cells have been studied in the light microscope with the use of antiactin (33, 6) and F-HMM (46, 47). These reports agreed for the most part concerning the localization of stained components, demonstrating fluorescence above background in chromosome-to-pole fibers and at the poles, and not in the interzone. Ultrastructural studies either were not done (46, 47) or were shown to be impossible on account of extensive deterioration of structure after preparation for immunofluorescence localization (6).

Actin *has* been identified in mitotic and meiotic spindles of several cell types by electron microscopy after glycerination and incubation with HMM (3, 15, 11, 16, 24, 12). In one case, 6-nm fibers were reported in spindles of glycerinated cells without addition of HMM (16).

The procedures described in this study were developed to determine the distribution of actin in cells prepared identically for both light and electron microscopy. We chose to use S-1 rather than HMM for fluorescence studies because of its

smaller size (120,000 vs. 340,000 daltons for HMM; reference 31) and its homogeneity on sodium dodecyl sulfate (SDS) polyacrylamide gels (e.g., reference 52). Precautions were taken to eliminate nonspecific interactions of F-S-1 with cellular structures by removal of overcoupled fractions. By fluorescence and electron microscopy, purified F-S-1 was shown to bind to actin-like microfilaments specifically in both interphase and mitotic cells.

MATERIALS AND METHODS

All protein solutions were handled at 4°C unless otherwise stated.

Myosin Subfragments

Rabbit skeletal muscle myosin was purified by a modification of the technique of Szent-Györgyi (49). Rather than removing actin by precipitating actomyosin, ATP and $MgCl_2$ were added to final concentrations of 2 and 4 mM, respectively, and actin was pelleted by centrifugation for 3 h at 100,000 g.

S-1 was prepared as described by Weeds and Taylor (52), by digestion at 25°C of myosin filaments with 0.05 mg of α-chymotrypsin/ml (Sigma Chemical Co., St. Louis, Mo.; bovine, crystallized three times) in 0.12 M NaCl, 0.02 M sodium phosphate, pH 7.0, and 1 mM EDTA. After terminating the digestion with 0.1 mM phenylmethylsulfonyl fluoride, insoluble myosin fragments were removed by centrifugation at 100,000 g. S-1 was further purified by collecting the ammonium sulfate precipitate between 30 and 60% saturation while maintaining pH between 7.2 and 7.5. The precipitate was dialyzed exhaustively against 0.01 M Tris-HCl pH 7.5. Sucrose was added to 5%, and the solution was lyophilized. The resulting powder was stored at −20°C.

Samples of S-1 powder were suspended in and dialyzed against 0.03 M imidazole-HCl pH 7.0 and separated into two peaks on a 30 × 2.6-cm column of diethylaminoethyl(DEAE)-cellulose (Cellex D, Bio-Rad Laboratories, Richmond, Calif.) using a linear gradient of 0–0.12 M NaCl, as described by Weeds and Taylor (52). S-1 peaks 1 and 2 eluted at 28 and 47 mM NaCl, respectively. Column fractions comprising each peak were pooled, and peaks 1 and 2 were concentrated by precipitation with 60% saturated ammonium sulfate at pH 7.2–7.5, and then dialyzed exhaustively vs. 0.01 M Tris-HCl pH 7.5. HMM was prepared by the method of Pollard et al. (39).

Conjugation of S-1 to Fluorescein Isothiocyanate (FITC)

Two different methods of conjugation were used:

METHOD A: FITC (United States Biochemical Corp., Cleveland, Ohio) was weighed into a glass vial for a final ratio of 25 μg of FITC/mg protein (53).

25-30 mg of S-1 peak 2, at 8-10 mg/ml in 0.01 M Tris-HCl, pH 7.5, was added with stirring at 4°C. The pH of the reaction mixture was monitored for 1 h and adjusted to 7.5-7.8 with 0.1 N NaOH if necessary. The vial was then sealed and the reaction allowed to continue for 5 h. After conjugation, the pH was checked to assure that it had remained in the desired range. Excess fluorescein was immediately removed by gel filtration in 0.01 M imidazole-HCl pH 7.0 on a 30 × 1.5-cm column of G-25 Sephadex (medium grade). Unbound fluorescein moved slowly as a diffuse band. The conjugate eluted with the void volume and was recognized as the first visible, yellow band.

METHOD B: FITC was dissolved in a small amount of buffer and S-1 peak 2 (8-10 mg/ml of 0.01 M Tris-HCl pH 7.5) was added with stirring, at room temperature (35). The final FITC concentration was 25 μg/mg of protein. The pH of the reaction mixture was adjusted to 7.5-7.8 during the 1-h conjugation period by addition of 0.1 N NaOH. Unreacted FITC was removed by gel filtration on G-25 Sephadex equilibrated with 0.01 M imidazole-HCl pH 7.0.

Chromatography of F-S-1

The gel filtration eluant was applied to a 5 × 1.5-cm column of DEAE-cellulose (the same batch as that used for separation of S-1 into 2 peaks) which had been previously equilibrated with 0.01 M imidazole-HCl pH 7.0. Peaks of S-1 with increasing fluorescein-to-protein ratios were eluted with a step gradient ranging from 0 to 0.5 M NaCl buffered with imidazole (see Results for concentration increments used in particular experiments). The column was monitored at 278 and 495 nm with a Zeiss PM6 spectrophotometer. Peaks were collected and concentrated by adding ammonium sulfate to 60% saturation at pH 7.2-7.5. Samples were dialyzed exhaustively vs. 0.01 M Tris-HCl pH 7.5.

Actin

Actin was purified from rabbit skeletal muscle according to the following procedure (D. J. Hartshorne, personal communication). KCl-phosphate-extracted back and leg muscle mince (49) was stirred for 30 min at 4°C in 0.4% NaHCO$_3$, 0.1 mM CaCl$_2$, filtered through cheesecloth, and suspended in 0.01 M NaHCO$_3$, 0.01 M Na$_2$CO$_3$, and 0.1 mM CaCl$_2$. After 10 min the solution was diluted with 10 vol of distilled water at 22°C and squeezed through cheesecloth. The residue was extracted five times with a total of 10 vol of cold acetone. After each extraction, the residue was collected on cheesecloth. The residue was finally dried overnight at room temperature and stored at −20°C.

Actin was extracted by stirring with 20 ml of 4°C, CO$_2$-free distilled water per gram of powder. Actin in the filtrate was polymerized at room temperature by the addition of NaCl and MgCl$_2$ to 10 and 0.7 mM, respectively. Regulatory proteins were extracted with 0.6 M

KCl for 1 h at 4°C, and fibrous actin (F-actin) was pelleted by centrifugation for 3 h at 100,000 g.

For negative stains, the actin was depolymerized by 72-h dialysis vs. 0.2 mM CaCl$_2$, 0.2 mM ATP, and 5 mM Tris-HCl pH 8.0, and repolymerized with 0.1 M KCl, 0.01 M potassium phosphate buffer pH 8.0. This resulted in less aggregated F-actin than was obtained without repolymerization.

Gel Electrophoresis

SDS-polyacrylamide gels were run and stained according to the procedure of Fairbanks et al. (8).

Protein Determination

Protein concentrations of conjugated S-1 (F-S-1) were estimated by the micro-biuret method (28) with bovine albumin (BSA) as standard. The micro-Kjeldahl method was used, assuming 16% nitrogen, to determine BSA concentration and to assure that the fluorochrome did not interfere with the color change associated with the biuret reaction.

ATPase Activity

Actin activation of the Mg^{++}-ATPase activity of S-1 and F-S-1 samples was assayed in a total volume of 2 ml containing 2.5 mM MgCl$_2$, 25 mM Tris-HCl, pH 7.5, and 2.5 mM ATP, for 5 or 30 min at 25°C (23). Inorganic phosphate was determined by the method of Fiske and SubbaRow (9).

Fluorescein-to-Protein (F/P) Molar Ratio

The molecular weight of S-1 peak 2 was calculated as follows. Polyacrylamide gels of the sample were scanned at 550 nm with a Beckman model DUR spectrophotometer (Beckman Instruments, Inc., Cedar Grove, N. J.), and a Gilford 2000 recorder (Gilford Instrument Laboratories Inc., Oberlin, Ohio). Light chain stoichiometry was estimated from these scans. Assuming chain weights of 90,000 daltons for the heavy chain fragment (32) and 21,000, 19,000, and 17,000 for the three light chains (51), a value of 120,000 was obtained for the molecular weight of S-1 peak 2. The molar extinction coefficient used for bound fluorescein was 4.25 × 10^4 cm^{-1} (50).

Cell Culture

Rat embryo (RE) cells were obtained from a primary culture of whole embryos. The cells were frozen after one passage. Each vial of cells was thawed and maintained in culture for about 3 wk, at which time the cells were discarded and a new vial was thawed. Cells were grown in Dulbecco's Modified Eagle's medium (DME; H-21, (Grand Island Biological Co. (GIBCO), Grand Island, N. Y.) supplemented with 10% calf serum and 50 μg of Gentamicin (Schering Corporation, Kenilworth, N. J.)/ml.

Rat kangaroo (Pt K1) cells (CCL 35, American Type

Culture Collection, Rockville, Md.) were grown in DME with 10% fetal calf serum, 50 μg of Gentamicin/ml, and 1 mM sodium pyruvate.

Cultures were maintained in a humid, 5% CO_2 atmosphere at 37°C. Every 3-4 days, cultures were removed from their plastic dishes (Falcon Plastics, Div. of Bio-Quest, Oxnard, Calif.) with 0.05% trypsin-EDTA solution (GIBCO) and replated into fresh medium. A coating of poly-L-lysine (av mol wt ~4,000, 0.05% in water) was sometimes used to anchor cells onto plastic or glass surfaces during glycerination.

Light Microscopy

Cells grown on no. 1 glass cover slips were made permeable by a modification of the glycerol extraction technique of Goldman (18). The culture medium was replaced with 50% glycerol (vol/vol) in a modified standard salt solution (MSS) containing 50 mM KCl, 15 mM $MgCl_2$, and 7 mM potassium phosphate buffer at pH 7.0. After 5-10 min, this extracting solution was replaced for 5-10 min with 25% glycerol in MSS, and similarly for 12 and 5% glycerol in MSS. The cover slips were rinsed twice with MSS and placed in a humid chamber consisting of a piece of wet filter paper in a Petri dish. This allowed use of small volumes (50 μl) of F-S-1 for staining. F-S-1 was diluted to 0.5 mg/ml (unless otherwise indicated) in standard salt solution (SSS: 50 mM KCl, 5 mM $MgCl_2$, 7 mM potassium phosphate, pH 7.0) and placed on the cover slips for 10-20 min. The cover slips were then returned to Petri dishes, where they were rinsed once with SSS and five times over a period of 15 min with MSS. The cover slips were supported on glass chips on a glass slide to avoid crushing the cells, were sealed (17), and then observed in MSS. A similar protocol was followed for control experiments, changing only the staining solutions and rinsing as indicated below. All extraction and labeling procedures were carried out at room temperature. Slides were generally studied immediately; however, several cover slips were examined after storage for 24 h at room temperature in MSS containing 50 μg of Gentamicin/ml. There was no detectable change in the phase-contrast or fluorescence images of these specimens.

A rapid, one-step glycerol extraction technique was used in parallel with most of the experiments described below, and yielded identical results. The medium was carefully removed from cells in a petri dish and replaced with 50% glycerol in MSS. After 1-2 min, the glycerol solution was drained as completely as possible and replaced with MSS. 2 min later, F-S-1 was added to the cells for 1-2 min, followed by several washes in MSS. This procedure resulted in phase-contrast and fluorescence images identical to those obtained with the longer (approximately 1 h) extraction protocol. With this rapid procedure, SSS or Dulbecco's phosphate-buffered saline (PBS: 0.14 M NaCl, 2.4 mM KCl, 8 mM Na_2HPO_4, 1.6 mM KH_2PO_4, 1 mM $CaCl_2$, and 0.5 mM $MgCl_2$) could be used in place of MSS and gave identical results. For

ease of comparison, all micrographs presented in this report were from cells prepared with the longer protocol with MSS, except for two electron micrographs (Figs. 11a and b).

Consistent fluorescent labeling of cells extracted with the rapid one-step procedure was obtained with F-S-1. When F-HMM, which is over twice the molecular weight of F-S-1, was used, fluorescent labeling of intracellular fibrous structures was often limited to areas where large holes could be seen in the cell surface. This appeared to result from limited diffusion of the larger myosin fragment and could sometimes be corrected by doubling the extraction, rinsing, and F-HMM incubation times.

Photomicrographs were made with a Zeiss Photomicroscope III equipped with a IIIRS epifluorescence condenser or phase-contrast microscopy. Zeiss objectives used are described in the figure legends. Illumination for fluorescence micrographs were provided by a DC powered HBO 100-watt mercury burner or an XBO 75-watt xenon arc. A Zeiss BG38 (red suppressing) filter remained between light source and specimen at all times. Excitation wavelengths ranged from 330 to 550 nm with maximum transmission at 400 nm (Zeiss BG12 filter). The dichroic beam-splitter cutoff was 510 nm. Viewing wavelengths were above 519 nm (Zeiss barrier filter 50). Plus-X film rated at DIN 27 was developed in Diafine (Acufine Inc., Chicago, Ill.).

Electron Microscopy

Cells in 35-mm plastic Petri dishes were treated as described above (see Light Microscopy), except that staining with F-S-1, S-1, or HMM was done directly in the dish for 15 min. After the final rinse with MSS, the cells were fixed with 1% glutaraldehyde in PBS for 30 min, rinsed three times with PBS, postfixed for 30 min with 1% osmium tetroxide in PBS, and rinsed three times with PBS. The cells were dehydrated through 70, 95%, and absolute ethanols and embedded in Epon-Araldite. The hardened plastic containing the cells was removed from the Petri dishes. Mitotic cells were located with a Leitz inverted microscope and marked with a slide marker (Ebtec Corporation, Agawam, Mass.). These regions were cut out and glued onto the ends of prepolymerized BEEM (Better Equipment for Electron Microscopy, Inc., Bronx, N.Y.) capsules. Flat-embedded interphase cells were also mounted on BEEM capsules. Thin sections were made parallel to the growth substrate, beginning in the region of cell-substrate contact, on an LKB Ultrotome and were collected on uncoated, 300-mesh copper grids (22). Sections were stained with uranyl acetate (30) and lead citrate (43) and observed with a Philips 201C electron microscope.

Negative stains were made by applying a drop of F-actin (see above) at approximately 0.1 mg/ml in 0.1 M KCl, 0.01 M potassium phosphate buffer pH 8.0 to Formvar/carbon-coated 200-mesh copper grids. After 30 s, excess actin was removed with filter paper. Before the grid was dry, a drop of F-S-1 at 0.2 mg/ml was placed on

the grid. 30 s later the excess was removed and the grid was rinsed twice with the actin buffer, once with aqueous 2% uranyl acetate, and, finally, negatively stained with uranyl acetate.

RESULTS

Preparation of S-1 and F-S-1

Rabbit skeletal muscle myosin S-1 was separated into two fractions by ion exchange chromatography. The fractions were similar to those described previously (54, 52). The first peak consisted primarily of heavy chain and A1 light chain, the second of heavy chain, A2 light chain, and a small amount of A1 chain (Fig. 1). We chose the second peak for conjugation experiments. Preliminary results indicate that conjugated samples of the first S-1 peak give results identical to those observed for second peak conjugates.
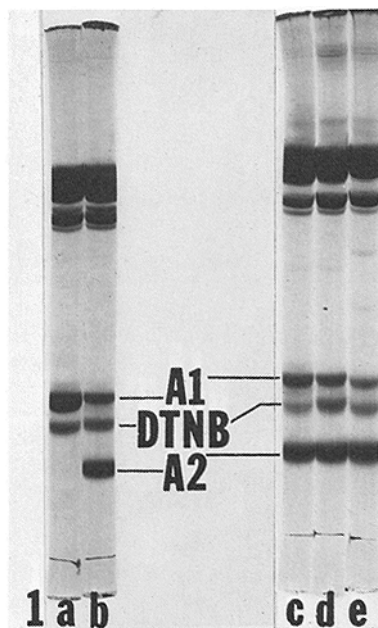
FIGURE 1 SDS-polyacrylamide gel profiles of S-1 peaks 1 (a) and 2 (b) and of F-S-1 peaks α (c), β (d), and γ (e). 5.6% gels loaded with 30 μg of protein. The myosin light chains are labeled (A1, DTNB, and A2). The similarity between b and c, d, and e indicates that separation of peaks α, β, and γ on DEAE is a function of the number of bound fluorescein molecules. In our S-1, some DTNB light chain was always present after chymotryptic cleavage. Other laboratories have not reported the presence of this chain (54, 52). This may be due to differences between the enzyme used here and that used by others (54, 52).

TABLE I

Characteristics of F-S-1 Conjugates

Peak	Gradient position*	Molar ratio (F/P)	SA retained‡	Average time for photographic exposure§
			%	s
α	0.05 M NaCl	1.0	67	75
β	0.07 M NaCl	2.0	55	33
γ	0.10 M NaCl	2.5	37	17

* Buffered with 0.01 M imidazole-HCl pH 7.0.

‡ Relative to SA of unlabeled S-1 peak 2. See Fig. 5.

§ Spot meter area centered on a fluorescent fiber. All exposure settings held constant except time. 20 measurements were made for each peak.

S-1 peak 2 was conjugated according to method A (see Materials and Methods) for most experiments and then applied to DEAE-cellulose. Elution with NaCl steps of 0.05, 0.07, and 0.10 M yielded peaks which were designated as α, β, and γ in the order in which they were eluted. The F/P molar ratios increased with each step in the gradient. There was some variation from one experiment to the next of the exact F/P ratio that eluted with a particular salt concentration. The range of F/P ratios within the gradient was, however, consistent. A representative example of one preparation is given in Table I and Figs. 1 and 2.

Many of the previous studies involving fluorescent labeling of proteins with FITC used pH values in a range of 8.5–9.5 for conjugation (e.g., references, 1, 53, 35, 45). In an attempt to reduce the possibility of denaturation of S-1 at high pH, we chose to carry out conjugation in a pH range of 7.5–7.8. After reaction under these conditions, the S-1-fluorescein complex moved as a single band on G-25 Sephadex. Separation on DEAE-cellulose resulted in superimposition of peaks resulting from protein and fluorochrome absorbance (see Fig. 2). To eliminate the possibility that the S-1-fluorescein interaction was noncovalent, the following experiment was performed. A sample of F-S-1 with a known F/P ratio was dialyzed for 24 h against 8 M urea. After denaturation, the F/P ratio (3.0) was virtually identical to the ratio before urea treatment (2.9), which indicated that fluorescein was bound in a stable manner to S-1 by our conjugation conditions.

Actin-Binding Studies on F-S-1 α, β, and γ

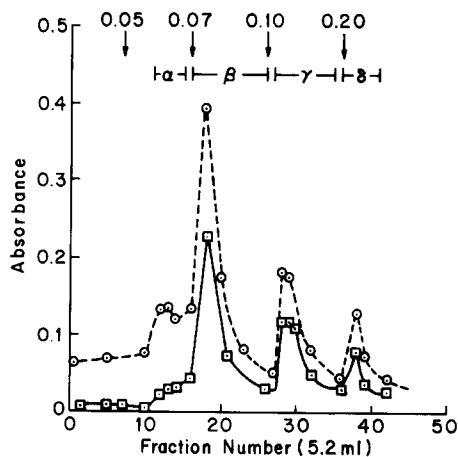To determine the capacity of the DEAE-purified F-S-1 to interact with actin, we tested for

FIGURE 2 A typical elution profile resulting in the separation of F-S-1 into fractions having different fluorescein to protein molar ratios. 21 mg of S-1 were reacted for 6 h with 525 μg of FITC (see Materials and Methods, conjugation method A). After removal of unbound fluorescein by gel filtration, the conjugate was applied to DEAE-cellulose and eluted with a step gradient consisting of the NaCl (molar) concentrations shown across the top of the figure. Fractions were pooled to yield samples designated α, β, and γ. 0.9, 3.2, and 1.3 mg of α, β, and γ, respectively, were recovered from the procedure. (○----○) Absorbance at 278 nm. (□——□) Absorbance at 495 nm.

decoration of actin and activation of ATPase activity.

Peak α eluted from DEAE at an ionic stength similar to that necessary for release of S-1 peak 2 from the same chromatographic medium. Peak α could therefore contain S-1 that was not coupled to fluorescein. Elution of peaks β and γ at higher ionic strengths indicated that these two peaks bound more tightly to DEAE, which was expected for S-1 with higher F/P ratios. Only these latter conjugate samples were used to check the ability of F-S-1 to decorate actin.

When rabbit skeletal F-actin was placed on an electron microscope grid and peak β or γ was added, arrowheads formed on the actin (Fig. 3), indicating that F-S-1 bound to actin in the correct configuration. Peak β was also shown to decorate microfilaments in glycerinated rat embryo cells (Fig. 4), demonstrating that conjugated S-1 interacted with nonmuscle actin-like microfilaments *in situ* as well as with muscle actin.

S-1 peak 2 retained 68% of the actin-activable ATPase activity of the original S-1 preparation (Fig. 5). In three experiments (one of which is

presented in Fig. 5), the DEAE-purified F-S-1 ATPase was activated by actin. The percentage of specific activity (SA) retained was always related to the order of elution, that is: $SA_\alpha > SA_\beta > SA_\gamma$. This finding parallels that of Wood et al. (53) who demonstrated decreasing activity of an antistreptococcal fluorescent reagent in proportion to an increasing number of bound fluorescein molecules. The retention of ATPase activity by peaks eluting after the unlabeled S-1 was eluted from the column is further evidence that conjugated S-1 can bind to actin in a physiologically significant and specific manner.

Light Microscopy of Interphase RE Cells Treated with F-S-1

Light microscope observations demonstrated that the fluroescent fibers seen in RE cells after glycerol extraction and staining with any of the F-S-1 fractions corresponded to stress fibers seen in phase contrast (Figs. 6, 7a and b). All three fractions yielded the same staining pattern. Stress fibers stained brightly, nuclear and nucleolar fluorescence were very low, and other cellular organelles did not fluoresce significantly (Figs. 8a, b, and c). A rough estimate of relative brightness of staining by peaks α, β, and γ was made by timing the exposures which were determined by the built-in photometer of the Zeiss Photomicroscope III. We consistently found that the required exposure time for cells stained with α was greater than that for cells stained with β which was greater than the time for cells stained with γ (see Table I).

When cells were incubated with 4 mM Mg^{++}-pyrophosphate and F-S-1, fluorescent stress fibers were not seen. Cells were very difficult to find in the fluorescence microscope field and were identifiable only by a blurred outline and diffuse cytoplasmic fluorescence (Fig. 8d). Thus, binding of F-S-1 to cytoplasmic actin was prevented by pyrophosphate, which is analogous to the situation in skeletal muscle. After rinsing with MSS, pyrophosphate-treated cells could be labeled with F-S-1 to yield a pattern of fluorescence identical to that seen in cells not treated with pyrophosphate.

Competition of F-S-1 binding by unlabeled S-1 also eliminated stress fiber fluorescence. Cells were exposed to a series of solutions which contained 0.1 mg of F-S-1/ml SSS and increasing concentrations of unlabeled S-1. With 0.1, 0.2, and 0.5 mg of unlabeled S-1/ml, the fluorescent image went from slightly to greatly reduced bright-
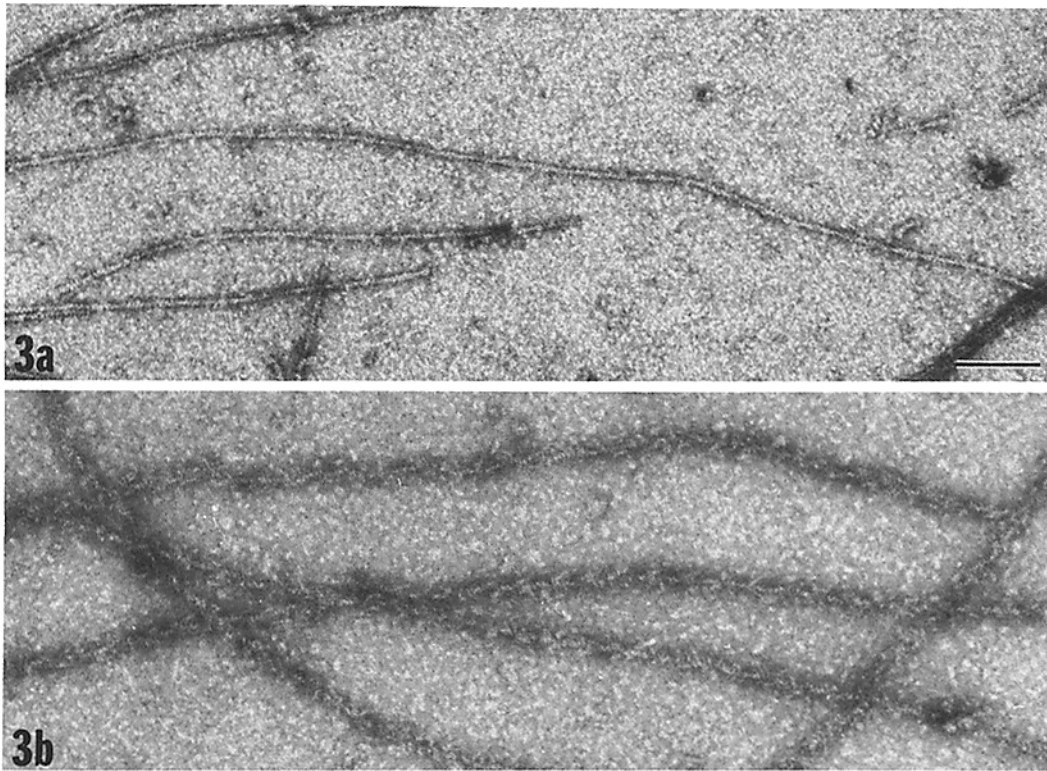
FIGURE 3 Electron micrographs of negatively stained (*a*) rabbit skeletal muscle actin and (*b*) actin plus F-S-1 (F/P = 2.5). After reaction with the F-S-1, arrowhead complexes are formed. Bar, 0.1 μm. × 110,570.

ness. When 1.0 mg of S-1/ml was present along with 0.1 mg of F-S-1-ml, the cells were still visible, but no stress fibers were seen. Cell margins and a faint image of the nucleus were the only visible remains of the staining pattern when cells were exposed to 0.1 mg of F-S-1/ml and 2.0 mg of unlabeled S-1/ml (Fig. 8*e*). Competition was successful for F-S-1 fractions with F/P ratios ranging from 1 to 3. Competition of F-S-1 with BSA over the same concentration range produced no change in the fluorescent image, indicating that a specific S-1 competition, and not a nonspecific protein-protein interaction, was occurring.

Light Microscopy of Pt K1 Cells Treated with F-S-1

When glycerol-extracted Pt K1 cells were incubated with F-S-1 and examined by fluorescence microscopy, stress fibers of interphase cells stained in a pattern similar to that seen in RE cells. Relative to stress fiber fluorescence, nuclear fluores-

cence was low. During mitosis, Pt K1 cells remain partially spread on the growth substrate, which facilitates examination of mitotic structures. F-S-1-treated Pt K1 spindle structures fluoresced above the background of cytoplasmic fluorescence. During metaphase, fluorescent chromosome-to-pole fibers were seen (Figs. 9*a* and *b*). In late anaphase or telophase cells, no fluorescence greater than background was seen in the interzone (Fig. 9*c*). A bright rim of cortical staining was often observed in mitotic cells (Fig. 9*g*). Both 4 mM Mg^{++}-pyrophosphate and S-1 competition experiments (conditions identical to those described for RE cells) eliminated spindle fluorescence. The only spindle structure that remained bright after these control incubations was the pole region. Interphase nuclei also remained visible after control incubations.

Owing to both the fading of fluorescence and the very low initial intensity of the control (pyrophosphate and S-1 competition) preparations, it was extremely difficult to locate mitotic cells by
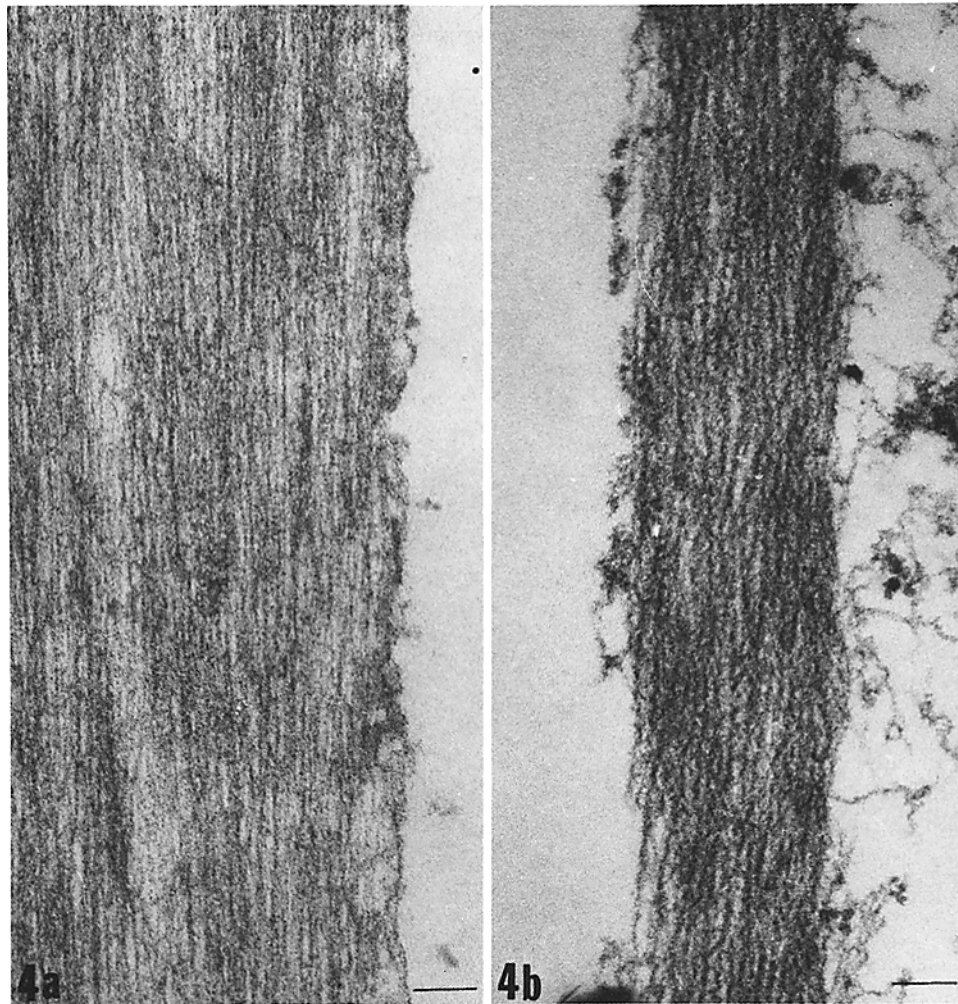
FIGURE 4 (a) Microfilament bundle seen in an electron micrograph of a thin section taken from a glycerinated rat embryo cell. × 86,410. (b) Microfilament bundle treated with F-S-1 (F/P = 2.0). The microfilaments are fuzzy in outline and more electron-dense than those seen in Fig. 4a. Bar, 0.1 μm. × 86,730.

epifluorescence alone. To insure that a reasonable number of cells were observed, the following steps were performed. Illumination with a halogen light source at low intensity in combination with the 546-nm green interference filter normally used for phase-contrast microscopy was outside the range of fluorescein-conjugate light absorption, which falls to zero above 545 nm (13). Under these conditions of illumination, cells in metaphase were located by phase-contrast microscopy. The same field was then viewed with epifluorescence microscopy. When located in this manner, spindles incubated with F-S-1 showed fluorescence above background in the chromosome-to-pole region (see Figs. 9a and b), whereas spindles in cells incubated for pyrophosphate or S-1 competition controls (at least 10 cells viewed in each case) showed fluorescence only at the poles.

Nonspecific Labeling of Cells due to Overcoupled S-1

Two methods were used to obtain F-S-1 samples with higher F/P ratios which resulted in overcoupled S-1 which no longer bound specifically to cellular actin.
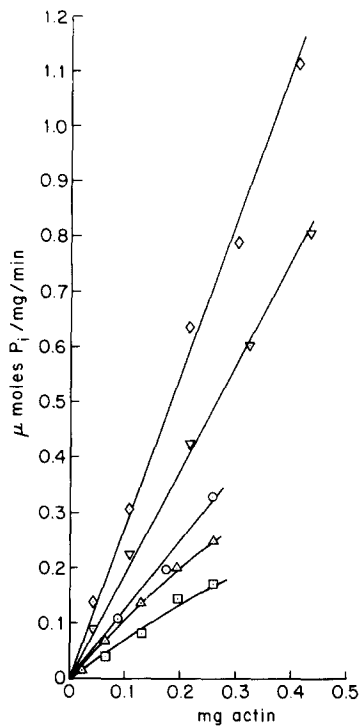
FIGURE 5   Actin activation of Mg^{++}-ATPase activity of S-1, S-1 peak 2, and F-S-1. The SA of peak 2 is 68% of that of the original S-1. Activities listed in Table I are relative to S-1 peak 2. (◇—◇) S-1. (▽—▽) S-1 peak 2. (○—○) F-S-1α. (△—△) F-S-1β. (□—□) F-S-1γ.

With the use of conjugation method A (see Materials and Methods), fractions with four to five fluorescein molecules per S-1 could be obtained by elution with 0.1–0.5 M NaCl. The protocol described yielded this material in quantities too small to allow assay of actin activation of Mg^{++}-ATPase for these samples. When glycerinated rat embryo cells were incubated with these fractions, stress fibers stained, although not so intensely as in cells stained with F-S-1 having lower F/P ratios. In addition, nuclei and nucleoli were very bright and general cytoplasmic fluorescence was more intense (see Fig. 8f). The staining reaction was not prevented by treatment with 0.004 M Mg^{++}-pyrophosphate, nor could competition with unlabeled S-1 be detected.

We have also prepared F-S-1 by room temperature conjugation for 1 h (as recommended by Nairn [35]; see method B, Materials and Methods) which retained 60% of the actin-activated ATPase activity of unlabeled S-1 (M.-J. Yerna,

personal communication) and which stained stress fibers brightly. When a sample of this rapidly labeled S-1 was purified on DEAE-cellulose, over 90% of the protein which eluted from the column had F/P ratios >4. These preparations stained stress fibers (Fig. 8f), but also caused other cellular material to fluoresce brightly. The spindle structures observed after reaction with overcoupled F-S-1 were similar to those described above for F-S-1 with F/P ratios of 1–2, but were much brighter (Figs. 9d–f). Pyrophosphate and unlabeled S-1 competition experiments were unsuccessful. Neither rabbit actin nor RE microfilaments in situ could be decorated by reaction with these overcoupled F-S-1 fractions.

Electron Microscopy of Mitotic Cells

GLUTARALDEHYDE-FIXED PT K1 CELLS: Mitotic spindles of nonglycerinated, glutaraldehyde-fixed cells were examined with the sole intent of determining whether or not microfilaments could be seen. A detailed ultrastructural study of glutaraldehyde-fixed Pt K1 cells in all stages of mitosis has been published by Roos (44). Pt K1 spindles contain numerous microtubules oriented along the long axis of the spindle. Microtubules were often found closely packed together but were sometimes far enough apart to allow visualization of ~4- to 6-nm diameter fibrillar material in between the large numbers of ribosomelike particles (Figs. 10a–c).

GLYCEROL-EXTRACTED RE AND PT K1 CELLS: Cells extracted with glycerol but not treated with S-1 or HMM were examined. Relative to cells fixed directly with glutaraldehyde, much of the matrix material of the spindle was removed. Microtubules were found in configurations similar to those seen in nonglycerinated cells. The fibrillar material (~4- to 6-nm diameter) was more prominent after glycerination, probably as a result of the decrease in amount of electron-dense material in the spindle matrix (Figs. 11 and 12). In many instances, discrete 4- to 6-nm microfilaments were seen in the spindle. These often followed paths parallel to microtubules, and in other cases appeared more randomly organized (Figs. 11 and 12).

S-1 AND HMM-TREATED PT K1 CELLS: After glycerol extraction and incubation with S-1 or HMM, decorated microfilaments were found in the spindle; undecorated microfilaments were not seen (Figs. 13 and 14). Arrowheads were best
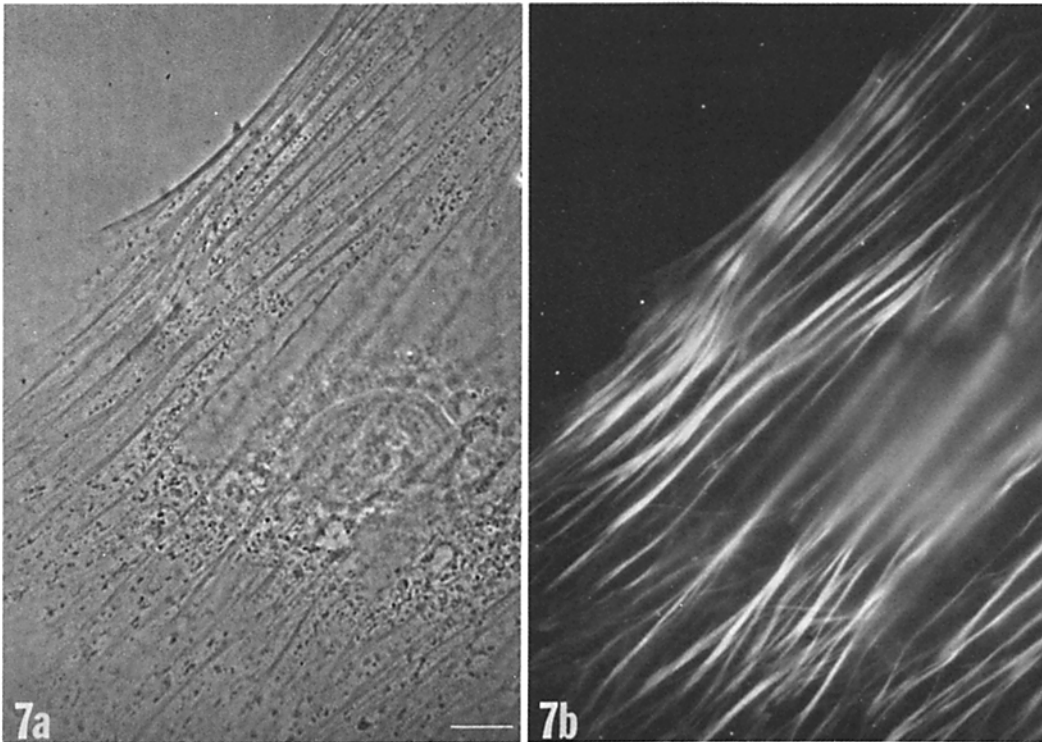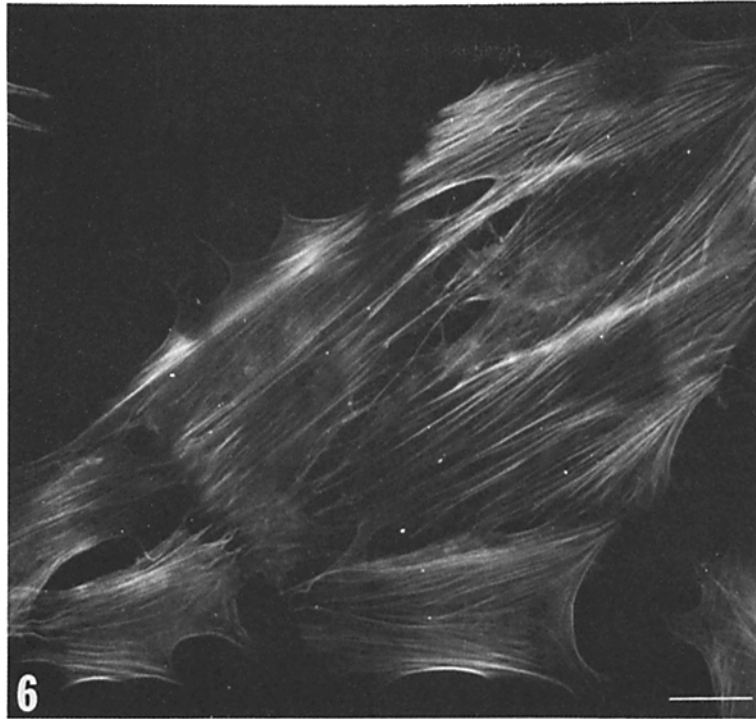
FIGURE 6   Fluorescence micrograph showing a field of RE cells treated with F-S-1 (F/P = 1.8). Stress fibers are the major labeled component in interphase cells. Bar, 40 μm. × 290 (Neofluar 16/0.4).

FIGURE 7   (a) Phase-contrast micrograph of a portion of a glycerinated RE cell that had been incubated with F-S-1 (F/P = 1.0). Note phase-dense fibers. (b) The same field as Fig. 7a viewed with epifluorescence illumination. Bright fibers correspond to phase-dense fibers in Fig. 7a. (a and b) Bar, 10 μm. × 820 (Phase planapochromat 63/1.4).
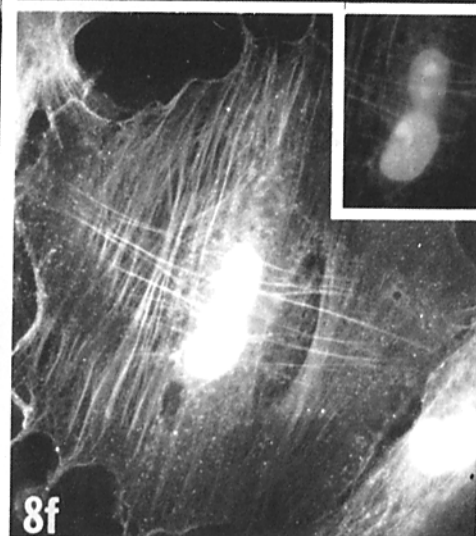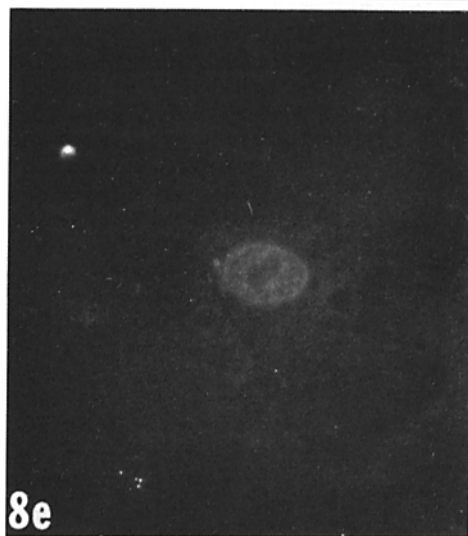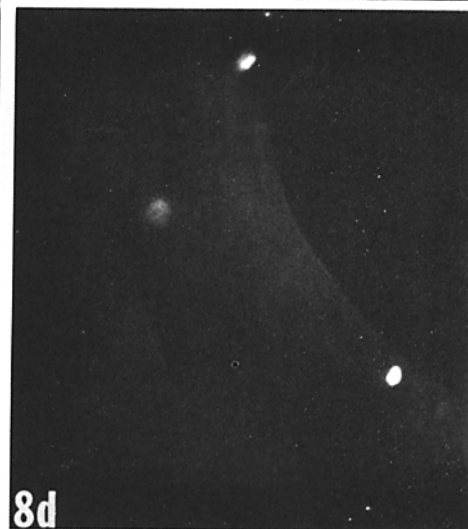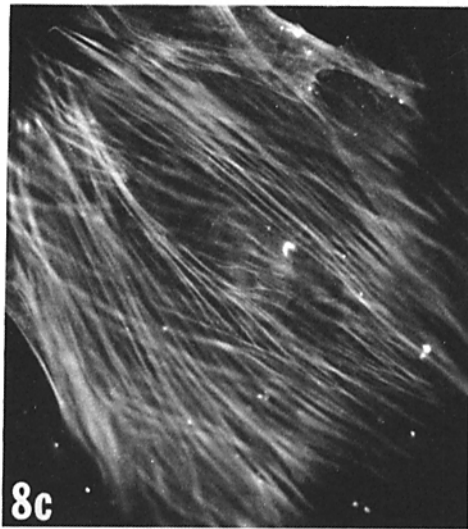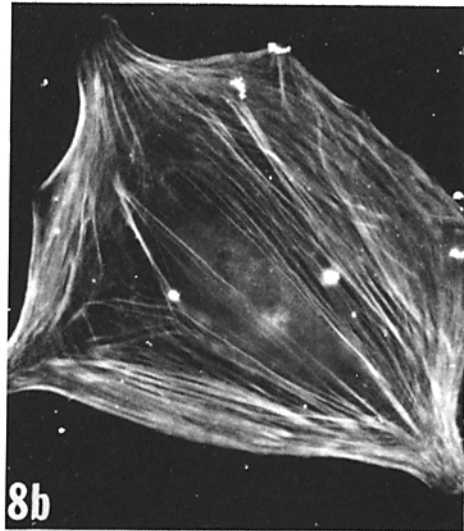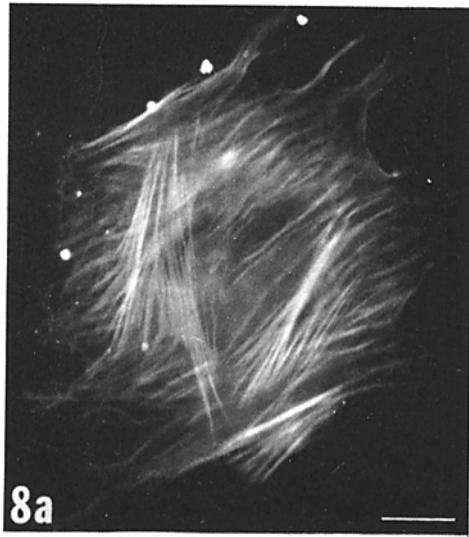
distinguished with S-1. The orientation and distribution of decorated microfilaments was similar to that of microfilaments in glycerinated cells not treated with myosin fragments; they were often associated with and sometimes parallel to microtubules. Decorated microfilaments were found in the chromosome-to-pole regions of metaphase and anaphase cells and in the interzones of anaphase cells. Decorated microfilaments were also found in the cortex of dividing Pt K1 cells (Fig. 14).

MICROFILAMENT-MICROTUBULE ASSOCIATION: In several sections, very close associations between microtubules and microfilaments were seen. Small groups of closely packed microtubules or individual microtubules which disappeared from the plane of the thin section frequently appeared to be continuous with microfilaments in glycerinated cells (Fig. 11 b) and with decorated microfilaments in cells treated with HMM or S-1 (Fig. 13), indicating a possible interaction between the two types of fibers.

DISCUSSION

Actin has been localized with light and electron microscopy by the addition of fluorescein-labeled rabbit skeletal myosin S-1 to glycerinated nonmuscle cells. Although some properties of S-1 are altered by coupling to fluorescein (e.g., the extent of activation of F-S-1 ATPase by skeletal muscle actin), it is possible to obtain labeled S-1 that reacts with actin in much the same manner as does unlabeled S-1. This is shown by the formation of arrowhead complexes with actin in negative stains, by decoration of microfilaments in thin sections, by prevention of binding by Mg^{++}-pyrophosphate, and by competition for the same actin-binding sites by unlabeled S-1. The cells used for these experiments were glycerinated and treated with F-

S-1 in exactly the same manner for light and electron microscopy. This makes possible a direct comparison of actin-containing structures at these two levels of resolution.

Wood et al. (53) showed that separation of fluorescein-labeled γ-globulin into fractions having limited ranges of F/P ratios was necessary to remove overcoupled antibody molecules. These overcoupled samples stained nonspecifically in the bacterial systems tested. We have demonstrated a similar effect. Glycerinated cells treated with overcoupled S-1 have diffuse cytoplasmic staining and intense nuclear fluorescence as well as fluorescent stress fibers. Moreover, the control experiments which demonstrate specific actin binding of F-S-1 with lower F/P ratios are not successful for overcoupled F-S-1. We therefore believe that it is important, in any study employing labeled myosin fragments, that these overcoupled fractions be removed in order to maintain the specificity of the light microscope probe.

Glycerination and incubation of mitotic Pt K1 cells with F-S-1 result in a fluorescent image of chromosome-to-pole fibers in the spindle. F-HMM (46, 47; our unpublished observations) and antibody to actin (33, 6) give similar results. We have attempted to visualize actin-like microfilaments by electron microscopy in positions corresponding to these fluorescent regions.

Electron micrographs of fixed (but not glycerinated) spindles do not unambiguously demonstrate the presence of microfilaments (see also references 2 and 34). Indeed, an individual microfilament would be difficult to visualize in any electron micrograph of sectioned animal cells. Microfilaments are most easily recognized when aggregated into bundles (e.g., reference 18). The distribution of 4- to 6-nm diameter fibrillar material in fixed specimens is similar to that of microfilaments

FIGURE 8 (a–c) RE cells incubated with F-S-1 with F/P ratios of 1.0, 2.0, and 2.5, respectively. Stress fibers fluoresce brightly. Nuclear fluorescence is low. The very bright spots represent cell debris. (d) RE cell incubated with F-S-1 (F/P = 1.0) in SSS with 4 mM pyrophosphate and then rinsed for 30 min with the same solution without F-S-1. The exposure and printing conditions were identical to those for Fig. 8a. Fluorescent fibers are no longer visible. For pyrophosphate experiments, increasing the KCl concentration to 0.1 M was found to produce more consistent results than using 50 mM KCl. This increase in KCl concentration did not affect other staining characteristics. (e) S-1 competition experiment. An RE cell incubated simultaneously with 0.1 mg of F-S-1 (F/P = 1.0)/ml and 2 mg of unlabeled S-1/ml. No fibers are seen and nuclear fluorescence is the main characteristic of these cells. (f) RE cells stained with overcoupled F-S-1 (F/P = 6.4). In addition to fluorescent fibers, the nuclear and general cytoplasmic fluorescence is higher than that seen in Fig. 8a–c. Inset is printed to show that nucleolar fluorescence is brighter than that of the nucleoplasm. (a–f) Bar, 20 μm. Epifluorescence, × 480 (Apochromat 40/1.0).
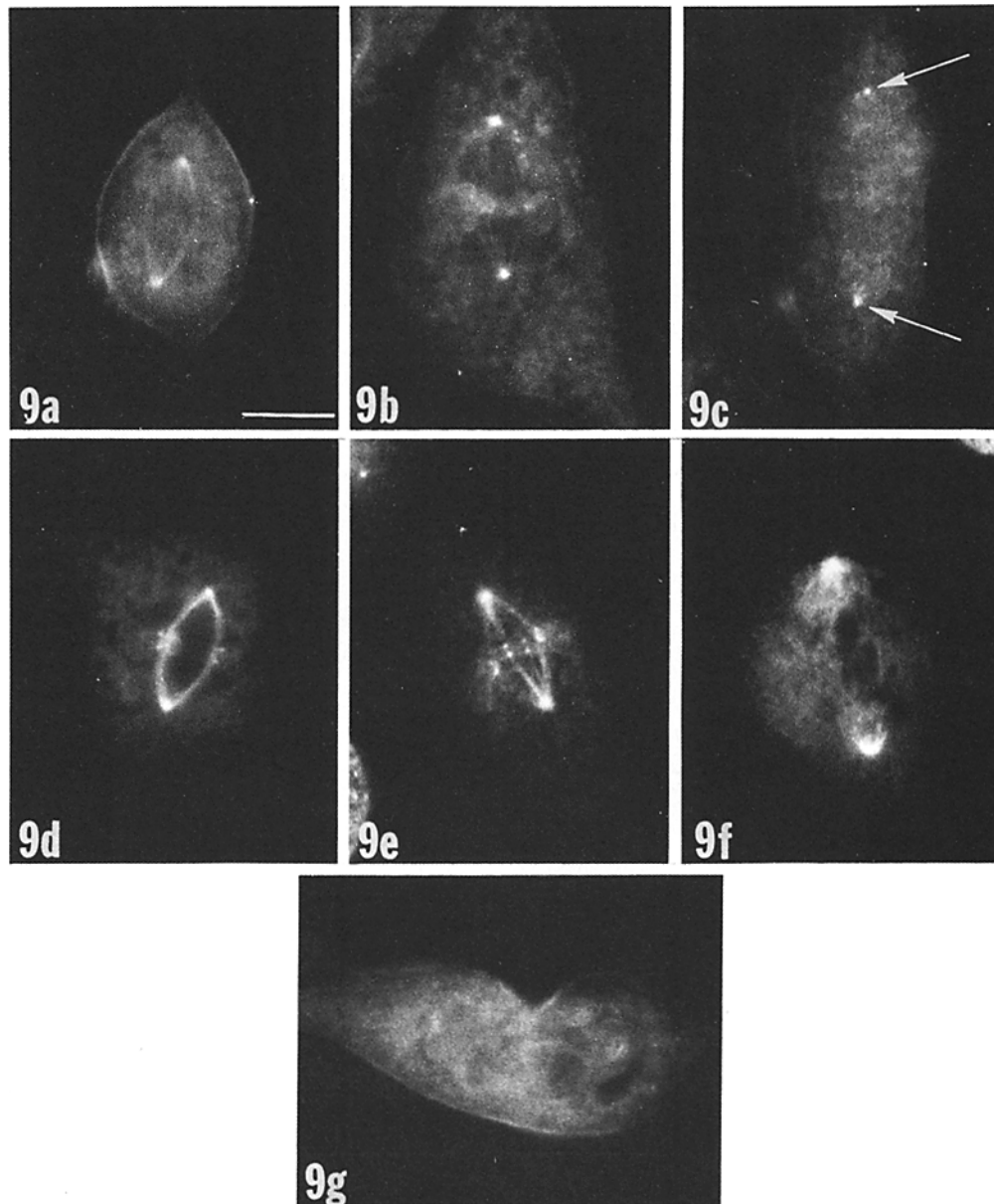
FIGURE 9 Glycerinated mitotic Pt K1 cells. (a and b) Metaphase cells incubated with F-S-1 (F/P = 2.1). Poles and chromosome-to-pole fibers are fluorescent. Some perichromosomal fluorescence is apparent in Fig. 9b but not in Fig. 9a. (c) Telophase cell treated as in Fig. 9a. No fluorescent fibers are seen in the interzone. Only the poles (arrows) fluoresce above background. (d and e) Metaphase cells incubated with overcoupled F-S-1 (F/P = 6.4). Poles, chromosome-to-pole fibers, and kinetochores fluoresce intensely: (f) Anaphase cell treated as in Fig. 9d. Short chromosome-to-pole fibers are seen, but no fibers fluoresce above background in the interzone. (g) Late telophase cell treated as in Fig. 9a. A rim of fluorescence above background level is seen at the cell periphery and the cleavage furrow. (a-f) Bar, 10 μm. Epifluorescence, × 1,200 (Planapochromat 100/1.25).
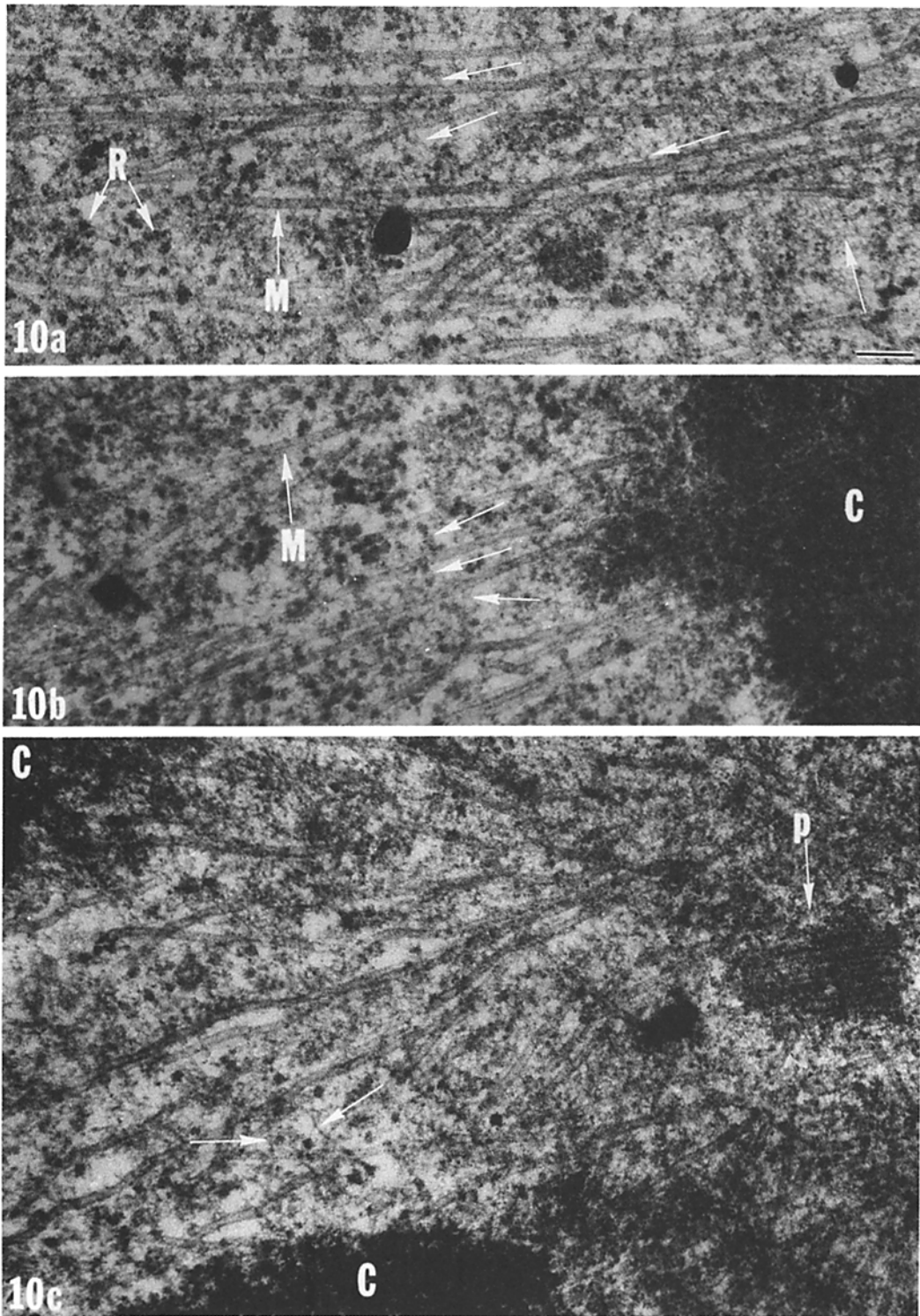
FIGURE 10 (a–c) Electron micrographs of Pt K1 cells fixed with glutaraldehyde without prior glycerination. Microtubules (M) running from chromosomes (C) to poles are surrounded by a dense matrix including ribosome-like particles (R). Where this matrix is less dense, fibrillar material is often seen (arrows) between the microtubules. This fibrillar material has a diameter of ~4–6 nm and is seen only when its long axis runs approximately perpendicular to the microtubules. In Fig. 10b the microtubules appear to insert into a chromosome. In Fig. 10c a centriole is seen as the pole (p) and is surrounded by a dense matrix. (a–c) Bar, 0.1 μm. × 82,500.
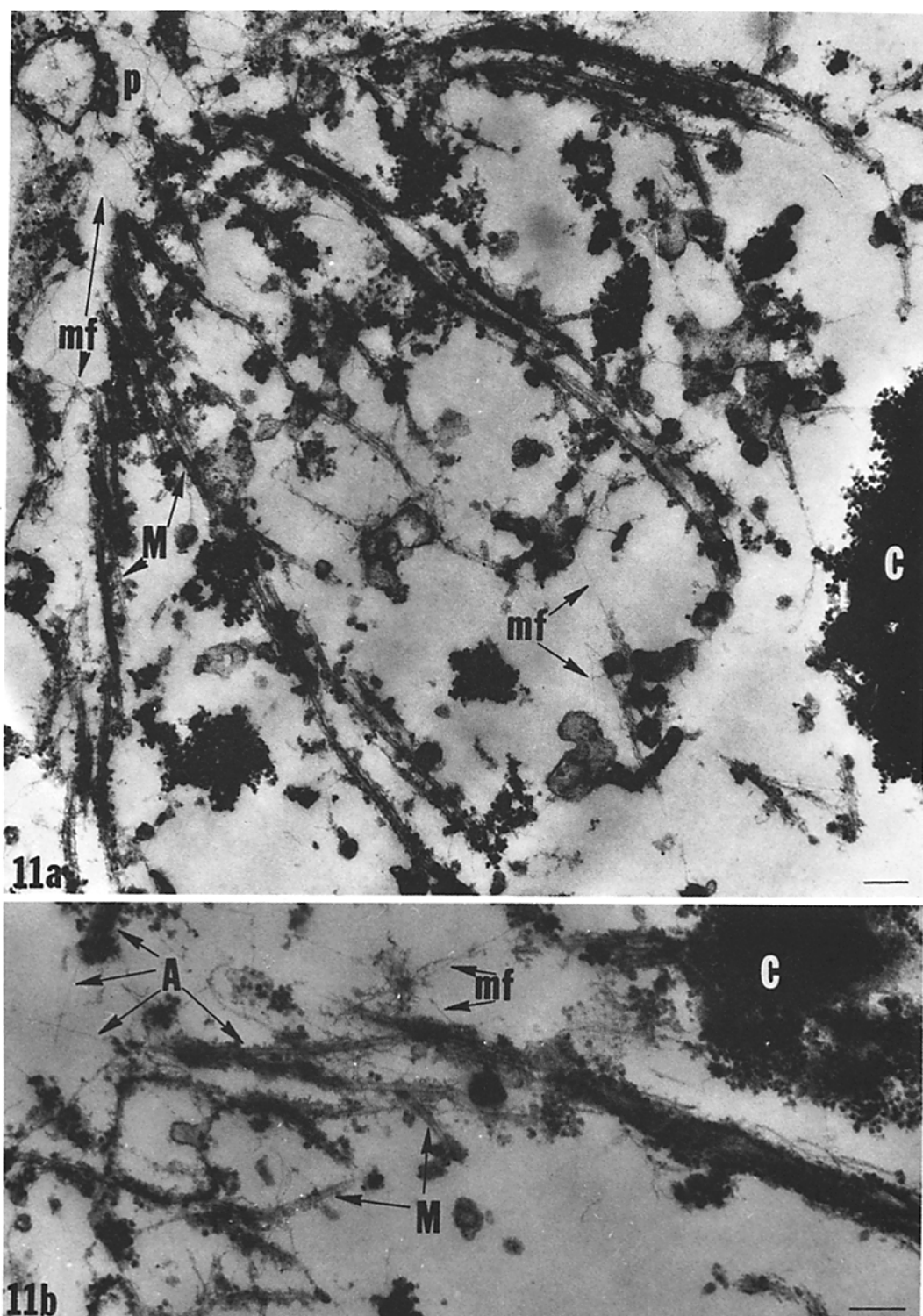
FIGURE 11 (a) Electron micrograph of an RE cell spindle after the one-step rapid extraction procedure (see Materials and Methods). Microtubules (M) run from the pole (p) region to the chromosomes (C). Many actin-like microfilaments (mf) are seen, often closely related to microtubules. Bar, 0.2 μm. × 33,600. (b) Interzone region of an anaphase RE cell prepared as in Fig. 11a. In at least two instances, point A, microfilaments project along the same path where microtubules go out of the plane of section. Bar, 0.2 μm. × 43,200.
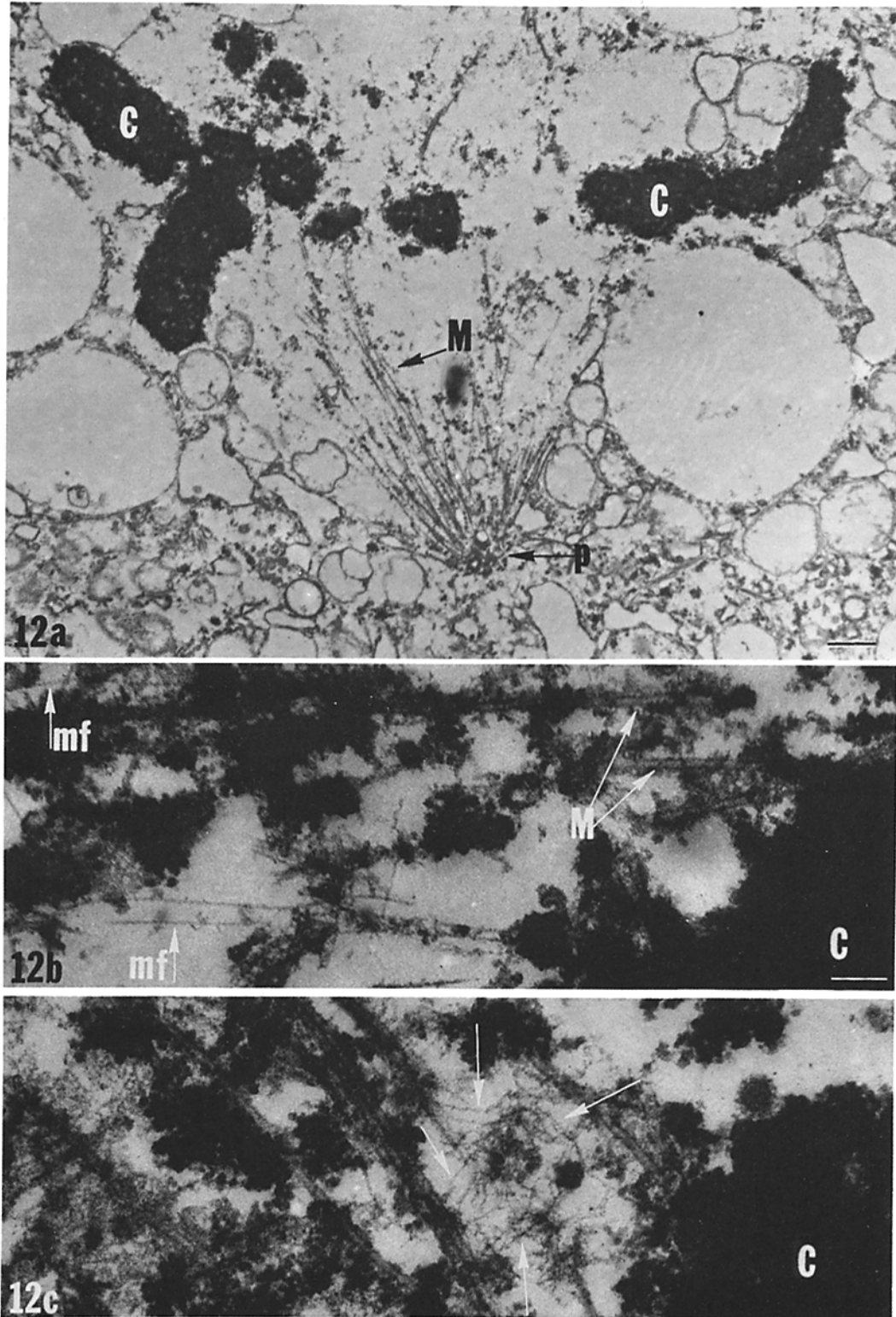
FIGURE 12 (a) Low magnification electron micrograph of a glycerol-extracted Pt K1 cell showing chromosomes (C) and microtubules (M) preserved in the chromosome-to-pole (p) region. Bar, 1 μm. × 7,750 (b) Higher magnification view of the chromosome-to-pole region of a cell treated as in Fig. 12 a. Note chromosome (C) and microfilaments (mf) running parallel to microtubules (M). (c) Another view of the chromosome-to-pole region showing randomly distributed microfilaments (arrows). (b and c) Bar, 0.1 μm. × 82,500.
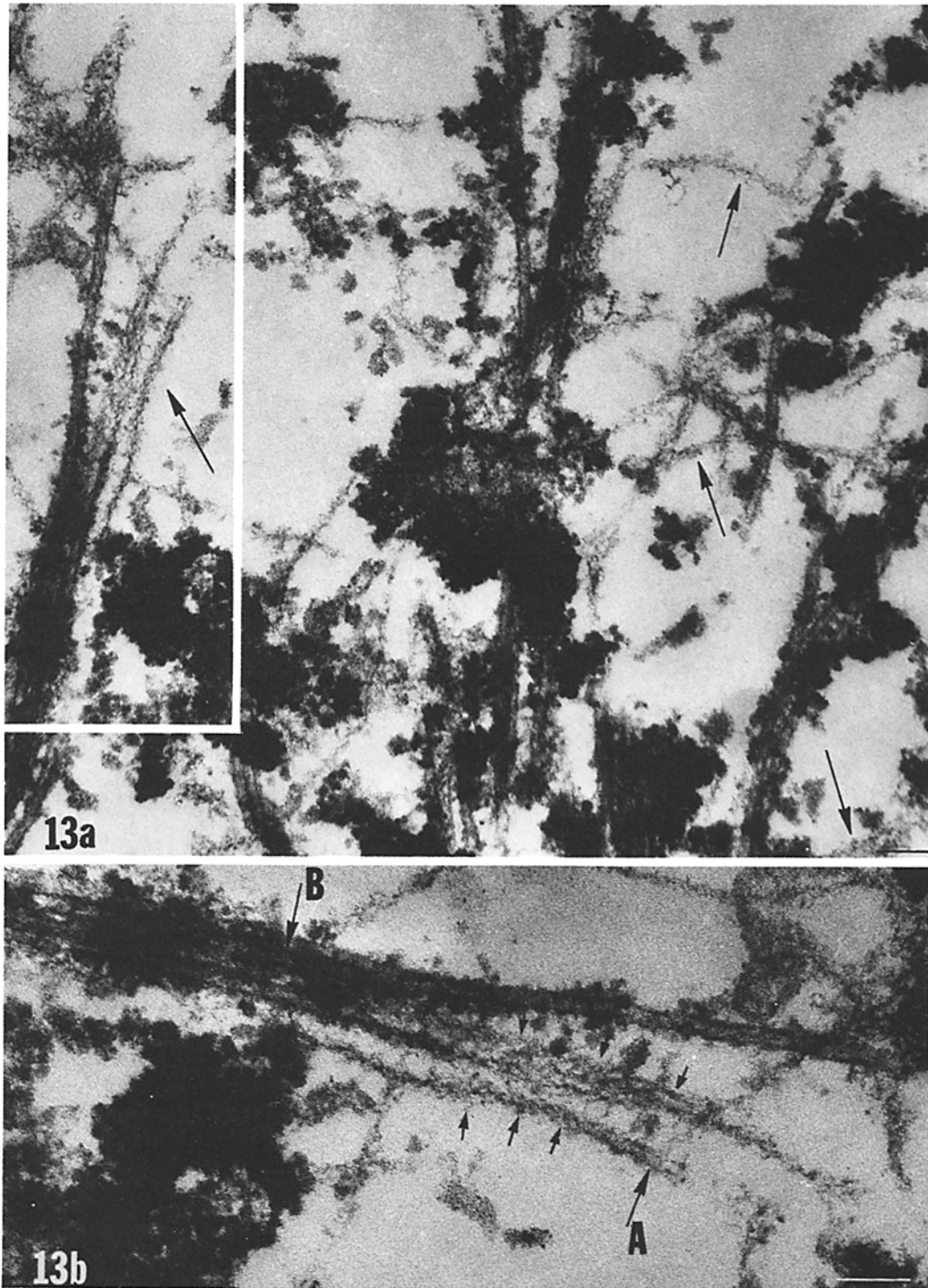
FIGURE 13 (a) Chromosome-to-pole region of a glycerol-extracted, HMM-treated Pt K1 cell. Decorated microfilaments (arrows) in some regions are seen running parallel to microtubules, and in other regions they appear to be randomly distributed. × 82,500. (b) A higher magnification view of the rectangular area indicated in Fig. 13a. In this region it appears as if microtubules leaving the plane of the thin section are continuous with decorated microfilaments. A points to a small region of a microtubule which appears to be continuous with a decorated microfilament (small arrows). B points to a group of three microtubules which appear to be continuous with a small bundle of decorated microfilaments (small arrows). Bar, 0.1 μm. × 115,500.
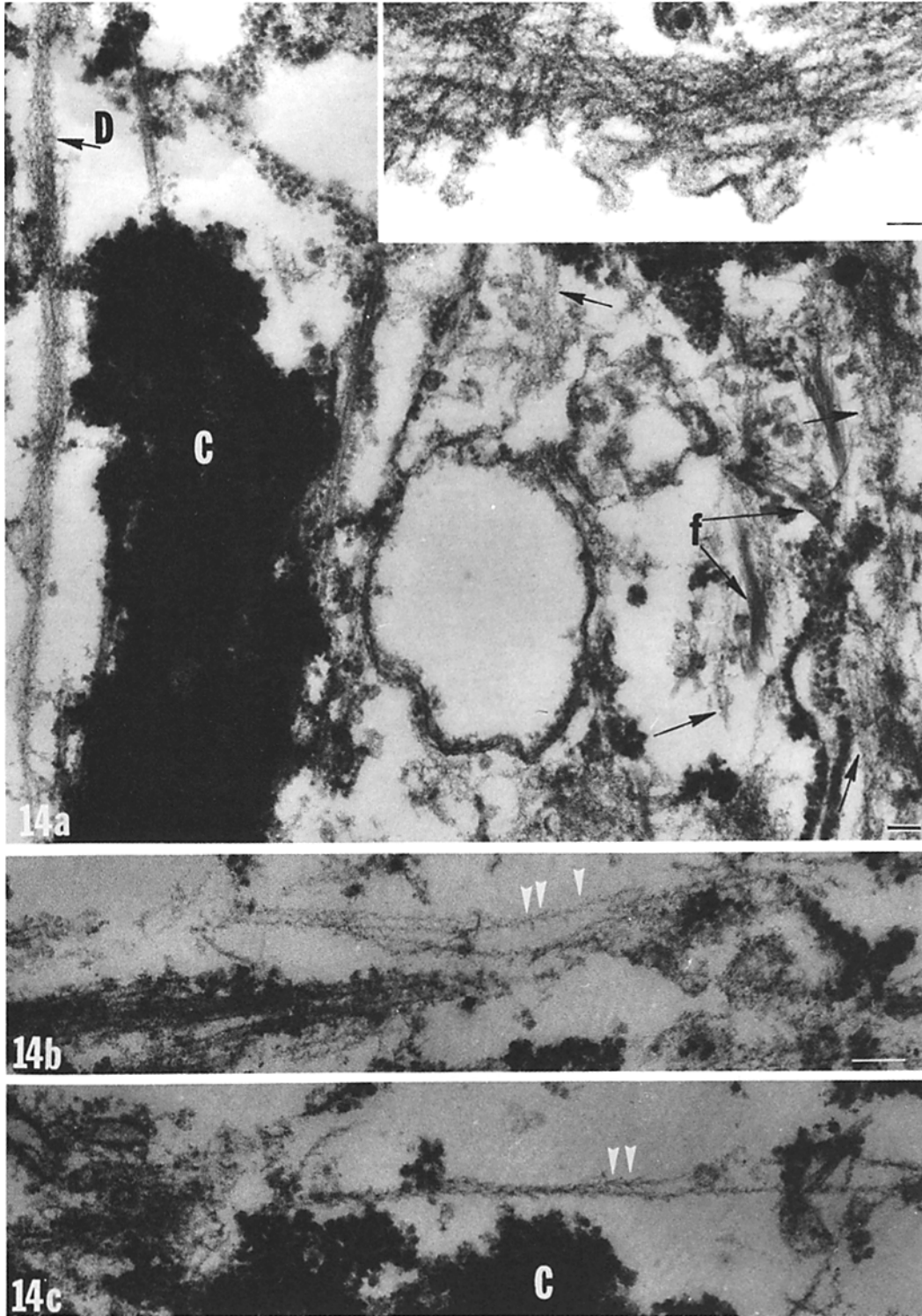
FIGURE 14   (a) An anaphase cell after glycerination and HMM incubation, showing decorated microfilaments (D) in the interzone region along one of the long arms of a chromosome (C). Decorated actin-like microfilaments are also evident in other regions of the cytoplasm and at the cortex (arrows). Masses of 100 Å filaments (f) are seen beneath the cortex. × 49,720. Inset is a higher magnification micrograph showing HMM decoration in a Pt K1 cell cortex. × 57,820. (b and c) Chromosome (C)-to-pole regions of glycerinated Pt K1 cells treated with S-1. Note decorated microfilaments containing arrowheads (arrows). Bar, 0.1 μm. × 82,500.

in glycerinated samples. The decrease in electron density of the spindle matrix after glycerol extraction appears to allow visualization of microfilaments (25).

Upon incubation with S-1 or HMM, microfilaments become thicker and fuzzy in outline (27, 19). The absence of undecorated microfilaments in samples treated with myosin heads indicates that thin filaments seen in only glycerinated samples are probably not microtubule protofilaments or other, previously undescribed types of fibers.

Actin-like microfilaments are found in the chromosome-to-pole regions and in quite large numbers near the poles (Figs. 11–14 and references 3, 15, 11, 10, 16, 24, 12). In addition, they are found in the interzone. Decorated microfilaments have also been reported in interzones of other cell types (11, 16). These latter observations appear to contradict the fluorescence results reported here and elsewhere (46, 47, 33, 6). If actin indeed does play a role in mitotic movements, one could speculate that once a chromosome has moved from its metaphase position, actin is no longer required in this region. As the chromosomes move closer to the poles, the actin remaining in the interzone may be redistributed and therefore decreased in amount. It is possible that the intensity of interzone actin-F-S-1 is simply not detectable by fluorescence microscopy over the ever present background fluorescence. The fact that background fluorescence in mitotic cells is reasonably high is not surprising, considering the presence of a cortical layer of actin. As shown in Fig. 14a, decorated microfilaments are present around the edges of the cell. This is the submembranous layer of microfilaments described in many types of animal cells (48, 55, 4, 18, 21).

Several reports indicate that decorated microfilaments are seen in glycerinated spindles after the addition of HMM (3, 15, 11, 16, 24, 12). Only one report exists showing that microfilaments are seen in glycerinated spindles of locust spermatocytes without addition of HMM (16). Visualization of microfilaments in spindles of glycerinated cells is an essential aspect in proving their existence in the spindle, because of the well-known ability of HMM to polymerize actin (7). Some types of S-1 may have the same effect (37). We have extended Gawadi's observations (15) to cultured rat embryo and Pt K1 cells by demonstrating the presence of actin-like microfilaments in glycerol-extracted spindles by long- and short-term extraction techniques (Figs. 11 and 12).

These glycerol extraction methods maintain not only the positions but also the birefringence of stress fibers in well-spread interphase cells (unpublished observations), and allow most of the actin to stay within the cells (21). Microfilament bundles seen in electron micrographs of glycerinated cells appear identical to bundles in directly fixed cells. In addition, actin filaments in striated muscle retain their appearance and position after glycerol extraction (25). These types of observations lead us to believe that glycerol extraction may be used reliably to study the distribution of actin-like microfilaments. The possibility does exist that some microfilaments might drift into the spindle or be polymerized there due to the extraction techniques. It may be noted, with regard to possible glycerol-induced polymerization artifacts (11), that immunofluorescence approaches not employing glycerination have demonstrated the presence of actin (33, 6) in specific spindle regions. The same regions contain actin-like microfilaments after glycerol extraction, as demonstrated by F-S-1 localization and the distribution of decorated microfilaments. Examination of cells extracted with cold acetone for 1 min followed by incubation with F-S-1 results in a pattern identical to that obtained with glycerination (unpublished observations). Extraction with cold (−20°C) acetone is a commonly used method for immunofluorescence localization. Identification of actin in the spindle by several methods is good evidence for its specific localization in that structure.

Regarding the possibility that actin might drift into the spindle, we have decreased the extraction time from several days (e.g., references 27 and 45) to 2–4 min to minimize the chance for such an occurrence. It is also interesting to note that microfilaments have been found in spindles of cells which possess very little actin in other regions of the cytoplasm (12).

A functional role for spindle actin has not yet been proved. In addition to showing the presence of actin-like microfilaments in spindles, it would be useful to determine whether or not there is a consistent polarity of the actin component relative to poles and chromosomes. Gawadi (16) and Forer and Jackson (12) have shown consistent polarities in a few, ideally visualized HMM-actin complexes. We have studied 60 HMM- or S-1-treated Pt K1 spindles and found the number of distinct arrowheads to be very low.

An observation that may shed light on the problems of spindle microfilament localization and

chromosomal movement is that of the close relationship between some decorated microfilaments and microtubules. Such microtubule-microfilament associations have been proposed on a theoretical basis (42, 10). The association becomes apparent during the analysis of thin sections of S-1- and HMM-treated Pt K1 cells. Spindle microtubules or bundles of microtubules which disappear from the plane of section appear to be continuous with decorated microfilaments. A possible explanation for these observations is that one or several microfilaments could be closely applied to the outer portion of the microtubule wall. If this association existed in cells fixed directly with glutaraldehyde, it would be impossible to resolve the microfilaments. Even a small number of actin-like microfilaments appear to be more than sufficient to produce the force required to move a chromosome to the pole (36, 10).

Our analyses of the properties of F-S-1 demonstrate that it can be used as a specific probe for actin localization in interphase and mitotic cells once overcoupled fractions have been removed. Although the fluorescence results indicate reasonable sensitivity, as shown by the ability to visualize the relatively small number of microfilaments in chromosome-to-pole regions of the mitotic spindle, there appears to be a lower limit to the detection of fluorescence above an expected background level, as demonstrated by the results concerning the interzone. The glycerination techniques employed provide a means for direct comparison of structure of the levels of light and electron microscopy. The growing body of evidence for actin in the mitotic spindle obtained by the several different methods for actin identification, along with recent evidence for myosin in the same regions of the mitotic apparatus (38, 14), is a convincing indication that an actomyosinlike contractile system may play a role in chromosome movement during mitosis and meiosis.

ADDENDUM

Because of the tremendous variations in electron density of chromosomes, ribosomes, microtubules, etc., relative to single microfilaments in the spindle region, some of the prints have backgrounds that are slightly darker than usual. This was necessary in order to optimize the information being presented.

While the manuscript was in preparation, I. M. Herman and T. D. Pollard presented an abstract in the *Biological Bulletin*, 1976 (**151**:413) concerning purification of rhodamine-HMM conjugates by ion exchange

chromatography, and T. E. Schroeder published a micrograph showing the possible association of microfilaments with interzone microtubules (1976. *Cell Motility*. R. Goldman, T. Pollard, and J. Rosenbaum, editors. Cold Spring Harbor Laboratory, Cold Spring Harbor, N. Y. p. 272).

REFERENCES

1. ARONSON, J. F. 1965. The use of fluorescein-labeled heavy meromyosin for the cytological demonstration of actin. *J. Cell Biol.* **26**:293-298.
2. BAJER, A., and J. MOLÉ-BAJER. 1969. Formation of spindle fibers, kinetochore orientation and behavior of the nuclear envelope during mitosis in endosperm. *Chromosoma (Berl.).* **27**:448-484.
3. BEHNKE, O., A. FORER, and J. EMMERSEN. 1971. Actin in sperm tails and meiotic spindles. *Nature (Lond.).* **234**:408-410.
4. BUCKLEY, I. K. 1974. Subcellular motility: a correlated light and electron microscopic study using cultured cells. *Tissue Cell.* **6**:1-20.
5. BUCKLEY, I. K., and K. R. PORTER. 1967. Cytoplasmic fibrils in living cultured cells: a light and electron microscope study. *Protoplasma.* **64**:349-380.
6. CANDE, W. Z., E. LAZARIDES, and J. R. McINTOSH. 1977. A comparison of the distribution of actin and tubulin in the mammalian mitotic spindle as seen by indirect immunofluorescence. *J. Cell Biol.* **72**:552-567.
7. COOKE, R., and M. F. MORALES. 1971. Interaction of globular actin with myosin subfragments. *J. Mol. Biol.* **60**:249-261.
8. FAIRBANKS, G., T. L. STECK, and D. F. H. WALLACH. 1971. Electrophoretic analysis of the major polypeptides of the human erythrocyte membrane. *Biochemistry.* **10**:2606-2609.
9. FISKE, C. H., and Y. SUBBAROW. 1925. The colorimetric determination of phosphorus. *J. Biol. Chem.* **66**:375-400.
10. FORER, A. 1974. Possible roles of microtubules and actin-like filaments during cell-division. *In* Cell Cycle Controls. G. M. Padilla, I. L. Cameron, and A.

M. Zimmerman, editors. Academic Press, Inc., N.Y. 319-336.

11. FORER, A., and O. BEHNKE. 1972. An actin-like component in spermatocytes of a crane fly (*Nephrotoma suturalis* Loew). I. The spindle. *Chromosoma (Berl.)*. **39:**145-173.

12. FORER, A., and W. T. JACKSON. 1976. Actin filaments in the endosperm mitotic spindles in a higher plant, *Haemanthus katherinae* Baker. *Cytobiologie*. **12:**199-214.

13. FOTHERGILL, J. E. 1969. Properties of conjugated serum proteins. *In* Fluorescent Protein Tracing. R. C. Nairn, editor. Williams and Wilkins Co., Baltimore, 35-60.

14. FUJIWARA, K., and T. D. POLLARD. 1976. Fluorescent antibody localization of myosin in the cytoplasm, cleavage furrow, and mitotic spindle of human cells. *J. Cell Biol.* **71:**848-875.

15. GAWADI, N. 1971. Actin in the mitotic spindle. *Nature (Lond.)*. **234:**410.

16. GAWADI, N. 1974. Characterization and distribution of microfilaments in dividing locust testis cells. *Cytobios*. **10:**17-35.

17. GOLDMAN, R. D. 1971. The role of three cytoplasmic fibers in BHK-21 cell motility. I. Microtubules and the effects of colchicine. *J. Cell Biol.* **51:**752-762.

18. GOLDMAN, R. D. 1975. The use of heavy meromyosin binding as an ultrastructural cytochemical method for localizing and determining the possible functions of actin-like microfilaments in non-muscle cells. *J. Histochem. Cytochem.* **23:**529-542.

19. GOLDMAN, R. D., and D. M. KNIPE. 1972. Functions of cytoplasmic fibers in nonmuscle cell motility. *Cold Spring Harbor Symp. Quant. Biol.* **37:**523-534.

20. GOLDMAN, R. D., E. LAZARIDES, R. POLLACK, and K. WEBER. 1975. The distribution of actin in non-muscle cells. *Exp. Cell Res.* **90:**333-344.

21. GOLDMAN, R. D., J. SCHLOSS, and J. STARGER. 1976. Organizational changes of actin-like microfilaments during animal cell movement. *In* Cell Motility. R. Goldman, T. Pollard, and J. Rosenbaum, editors. Cold Spring Harbor Laboratory, Cold Spring Harbor, New York. 217-245.

22. GOLDMAN, R. D., M.-J. YERNA, and J. A. SCHLOSS. 1977. The localization and organization of microfilaments and related proteins in normal and virus-transformed cells. *J. Supramol. Struct.* **5:**155-183.

23. HARTSHORNE, D. J., and H. MUELLER. 1969. The preparation of tropomyosin and troponin from natural actomyosin. *Biochim. Biophys. Acta.* **175:**301-319.

24. HINKLEY, R., and A. TELSER. 1974. Heavy meromyosin-binding filaments in the mitotic apparatus of mammalian cells. *Exp. Cell Res.* **86:**161-164.

25. HUXLEY, H. E. 1957. The double array of filaments in cross-striated muscle. *J. Biophys. Biochem. Cytol.* **3:**631-647.

26. HUXLEY, H. E. 1963. Electron microscope studies on the structure of natural and synthetic protein filaments from striated muscle. *J. Mol. Biol.* **7:**281-308.

27. ISHIKAWA, H., R. BISCHOFF, and H. HOLTZER. 1969. Formation of arrowhead complexes with heavy meromyosin in a variety of cell types. *J. Cell Biol.* **43:**312-328.

28. ITZHAKI, R. F., and D. M. GILL. 1964. A microbiuret method for estimating proteins. *Anal. Biochem.* **9:**401-410.

29. LAZARIDES, E., and K. WEBER. 1974. Actin antibody: the specific visualization of actin filaments in non-muscle cells. *Proc. Natl. Acad. Sci. U. S. A.* **71:**2268-2272.

30. LOCKE, M., and N. KRISHNAN. 1971. Hot alcoholic phosphotungstic acid and uranyl acetate as routine stains for thick and thin sections. *J. Cell Biol.* **50:**550-557.

31. LOWEY, S., H. S. SLAYTER, A. G. WEEDS, and H. BAKER. 1969. Substructure of the myosin molecule. I. Subfragments of myosin by enzymatic degradation. *J. Mol. Biol.* **42:**1-29.

32. MARGOSSIAN, S. S., and S. LOWEY. 1973. Substructure of the myosin molecule. III. Preparation of single-headed derivatives of myosin. *J. Mol. Biol.* **74:**301-311.

33. MCINTOSH, J. R., W. Z. CANDE, E. LAZARIDES, K. MCDONALD, and J. A. SNYDER. 1976. Fibrous elements of the mitotic spindle. *In* Cell Motility. R. Goldman, T. Pollard, and J. Rosenbaum, editors. Cold Spring Harbor Laboratory, Cold Spring Harbor, New York. 1261-1272.

34. MÜLLER, W. 1972. Elektronenmikroskopische Untersuchungen zum Formwechsel der Kinetochoren während der Spermatocytenteilunger von *Pales ferruginea* (Nematocera). *Chromosoma (Berl.)*. **38:**139-172.

35. NAIRN, R. C. 1969. Appendix. *In* Fluorescent Protein Tracing. R. C. Nairn, editor. The Williams and Wilkins Co., Baltimore. 3rd edition. 303-304.

36. NICKLAS, R. B. 1971. Mitosis. *In* Advances in Cell Biology. D. M. Prescott, L. Goldstein, and E. McConkey, editors. Academic Press, Inc., New York. **2:**225-297.

37. ONODERA, M., and K. YAGI. 1971. Studies on enzymatically active subfragments of myosin-adenosine triphosphatase. I. Preparation using chymotrypsin. *J. Biochem.* **69:**145-153.

38. POLLARD, T. D., K. FUJIWARA, R. NIEDERMAN, and P. MAUPIN-SZAMIER. 1976. Evidence for the role of cytoplasmic actin and myosin in cellular structure and motility. *In* Cell Motility. R. Goldman, T. Pollard, and J. Rosenbaum, editors. Cold Spring Harbor Laboratory, Cold Spring Harbor, New York. 689-724.

39. Pollard, T. D., E. Shelton, R. Weihing, and E. Korn. 1970. Ultrastructural characterization of F-actin from *Acanthamoeba castellani* and identification of cytoplasmic filaments as F-actin by reaction with rabbit heavy meromyosin. *J. Mol. Biol.* **50**:91-97.

40. Pollard, T. D., and R. R. Weihing. 1974. Actin and myosin and cell movement. *Crit. Rev. Biochem.* **2**:1-65.

41. Porter, K. R. 1976. Introduction: motility in cells. *In* Cell Motility. R. Goldman, T. Pollard, and J. Rosenbaum, editors. Cold Spring Harbor Laboratory, Cold Spring Harbor, New York. 1-28.

42. Rebhun, L. I. 1967. Structural aspects of saltatory particle movement. *J. Gen. Physiol.* **50**:223-239.

43. Reynolds, E. S. 1963. The use of lead citrate at high pH as an electron-opaque stain in electron microscopy. *J. Cell Biol.* **17**:208-213.

44. Roos, U. P. 1973. Light and electron microscopy of rat kangaroo cells in mitosis. *Chromosoma (Berl.)* **40**:43-82.

45. Sanger, J. W. 1975. Changing patterns of actin localization during cell division. *Proc. Natl. Acad. Sci. U. S. A.* **72**:1913-1916.

46. Sanger, J. W. 1975. Presence of actin during chromosomal movement. *Proc. Natl. Acad. Sci. U. S. A.* **72**:2451-2455.

47. Sanger, J. W., and J. M. Sanger. 1976. Actin localization during cell division. *In* Cell Motility. R. Goldman, T. Pollard, and J. Rosenbaum, editors. Cold Spring Harbor Laboratory, Cold Spring Harbor, New York. 1295-1316.

48. Spooner, B. S., K. M. Yamada, and N. K. Wessells. 1971. Microfilaments and cell locomotion. *J. Cell Biol.* **49**:595-613.

49. Szent-Györgyi, A. 1951. Chemistry of Muscular Contraction. Academic Press, Inc., New York. 2nd edition. 146-148.

50. Tengerdy, R. P., and C.-A. Chang. 1966. Optical absorption and fluorescence of fluorescent protein conjugates. *Anal. Biochem.* **16**:377-383.

51. Weeds, A. G., and S. Lowey. 1971. Substructure of the myosin molecule. II. The light chains of myosin. *J. Mol. Biol.* **61**:701-725.

52. Weeds, A. G., and R. S. Taylor. 1975. Separation of subfragment-1 isoenzymes from rabbit skeletal muscle myosin. *Nature (Lond.).* **257**:54-56.

53. Wood, B. T., S. H. Thompson, and G. Goldstein. 1965. Fluorescent antibody staining. III. Preparation of fluorescein-isothiocyanate-labelled antibodies. *J. Immunol.* **95**:225-229.

54. Yagi, K., and F. Otani. 1974. Studies of enzymatically active subfragments of myosin-adenosine triphosphatase. III. Separation of two components. *J. Biochem.* **76**:365-373.

55. Yamada, K. M., B. S. Spooner, and N. K. Wessells. 1971. Ultrastructure and function of growth cones and axons of cultured nerve cells. *J. Cell Biol.* **49**:614-635.